Macromolecules

pubs.acs.org/Macromolecules Article

Effects of Non-Electrostatic Intermolecular Interactions on the Phase Behavior of pH-Sensitive Polyelectrolyte Complexes

Lu Li, Samanvaya Srivastava,* Siqi Meng, Jeffrey M. Ting, and Matthew V. Tirrell*

Cite This: *Macromolecules* 2020, 53, 7835−7844 Read Online

ACCESS | Metrics & More | Article Recommendations | Supporting Information

ABSTRACT: Polyelectrolyte complexes (PECs) offer enormous material tunability and desirable functionalities, and consequently have found broad utility in biomedical and material industries. While poly(acrylic acid) (PAA) and poly(allylamine hydrochloride) (PAH) are a commonly used pairing, various aspects of the phase behavior of PAA−PAH complexes have not been sufficiently quantified. We present a comprehensive experimental study depicting the binodal phase boundaries for the PAA−PAH complexes prepared under acidic, neutral, and basic conditions using thermogravimetric analysis, turbidimetry, and optical microscopy. Under neutral and basic conditions, phase behaviors of the complexes were largely similar to one another and followed general expectations of PEC phase behavior, except for unusually high resistance to disruption of the complex with added salt. Stable complexes are observed up to 4 M NaCl concentrations. Under acidic conditions, strikingly different phase behaviors of the PAA−PAH complexes were observed. The polymer content in the complex phase increased initially, followed by an expected decrease as salt was added to the complexes. This behavior may result from a combination of associative phase separation of PAA and PAH chains, influenced by electrostatic interactions, and segregative phase separation, which can be ascribed to the influence of a combination of the hydrophobic interactions of the aliphatic polymer backbone and the interpolymer hydrogen bonding of unionized acrylic monomer units. Our systematic investigations over a range of pH detailing these discrepancies in the PAA−PAH phase behavior are expected to clarify the inconsistencies among the reports in the literature and provide the material design strategies for practical use of the PAA−PAH complexes and multilayer assemblies.

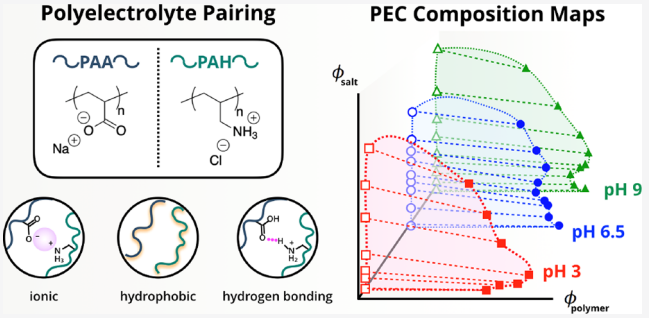

Mixing of oppositely charged polyelectrolyte solutions in aqueous solutions can result in associative phase separation of the polyelectrolytes leading to polyelectrolyte complexes (PECs).[1−5] With increasing awareness of striking parallels in biology, for example, the resemblance of PECs to membrane-less organelles emerging from spontaneous liquid−liquid phase separation[6,7] and material science as exceptionally tunable self-assembled structures,[8,9] PEC-based materials have received research interest across multiple disciplines. For instance, they have been employed as prototypes in reversible morphological phase transitions,[10,11] fabricated into hollow microcapsules and intertwined membranes by injection suspension or electron spinning,[8,12,13] and formulated into therapeutic delivery micelles[14−16] and biocompatible hydrogels.[9]

Several experimental[13,17−23] and theoretical studies[24−32] in recent years have investigated the thermodynamics[23,33,34] and kinetics[35,36] of polyelectrolyte complexation, focusing on the influence of electrostatic interactions and the concomitant entropic gains from the release of counterions upon complexation. Yet, only a handful of theoretical and simulation studies have investigated the influence of polymer−solvent interactions on the phase behavior of complexes.[37,38] Sato and Nakajima included the Flory interaction parameter χ to account for interaction between water and polyelectrolyte salt in the classical Voorn−Overbeek (V−O) theory[3] and deduced the limiting conditions of charge density and chain length for complexation.[39,40] Larson and co-workers extended the V−O theory[3] by incorporating the χ parameter between protonated poly(acrylic acid) and solvent molecules to explain the unusual high salt resistances of PECs measured in acidic environments.[37,41,42] Castelnovo and Joanny[32] and Kudlay et al.[25,26] adopted RPA-based methods to investigate the influence of the χ parameter on PEC phase behaviors and salt partitioning. A recent theoretical study by Rumyantsev et al. outlined a salt concentration−solvent quality diagram of PECs based on scaling laws.[38] Concomitantly, experimental investigations have begun to investigate the influence of

Received: April 28, 2020
Revised: July 30, 2020
Published: August 28, 2020

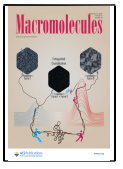

https://dx.doi.org/10.1021/acs.macromol.0c00999
Macromolecules 2020, 53, 7835−7844

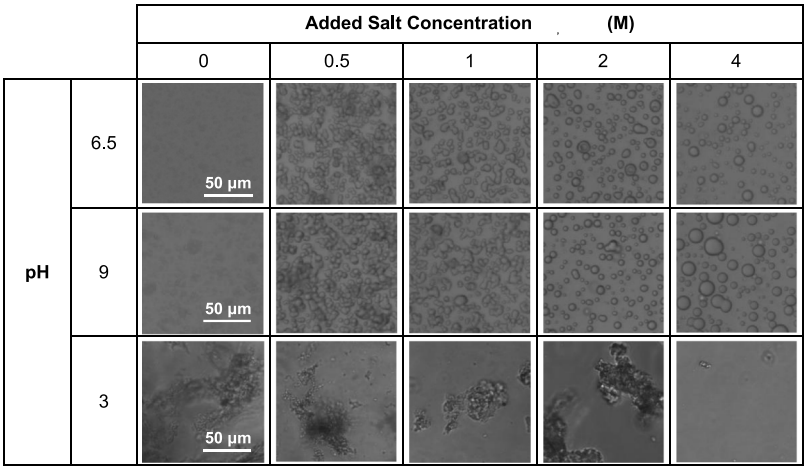

Figure 1. Representative micrographs of (rows 1 and 2) PAANa−PAH and (row 3) PAA−PAH complexes prepared at $C_{P,0}$ = 1% wt/v, $C_{S,added}$ = 0, 0.5, 1, 2, and 4 M NaCl, and pH = 6.5 (row 1), 9 (row 2), and 3 (row 3). At pH = 6.5 and 9, the morphology of the complexes changed from flaky precipitates to irregularly shaped droplets to spherical coacervate droplets with increasing $C_{S,added}$. At pH = 3, the complexes remained as flaky precipitates for all $C_{S,added}$ investigated. The scale bar is the same for all images.

parameters such as the unique chemical attributes of the individual polymers and solvent effects on complexation.[37,38,43] Sadman et al. have demonstrated mechanical tunability for poly(styrene sulfonate) and poly(4-vinyl pyridine) complexes by varying the hydrophobicity of the quaternized poly(4-vinylpyridine) through alkyne substitutions,[43] and Spruijt et al. included the χ parameter in calculations based on V−O theory to describe experimentally determined polymer contents in PECs.[44] More recently, the influence of polymer−solvent interactions on the phase behavior and complex morphology in PECs has been discussed in various polyelectrolyte systems ranging from natural polymers[45] to polypeptides[46] to synthetic polymers.[47,48] Prabhu and co-workers have reported a lower critical solution temperature for PEC systems[49] that were described in a mean-field theory formalism to identify the ranges of the solvent dielectric constant and the χ parameter justifying these observations.[50]

Despite the progress in the description of the influence of solvent interactions on complexation, detailed datasets describing the phase behavior quantitatively to illustrate the effect of hydrophobicity and other prevailing physical noncovalent interactions on polyelectrolyte complexation are still elusive. These more realistic aspects of complexation are essential to advance our current understanding of selecting polyelectrolyte pairs for PEC materials and to harness such materials into products and end-use technologies.

Here, we provide explicit quantitative descriptions of the binodal phase behavior of PECs comprising polyelectrolyte pairs with polarizable ionic groups on aliphatic backbones, resulting in accentuated hydrophobicity and hydrogen bonding interactions in conjunction with electrostatic interactions. The sodium salt of PAA (and its acid form, poly(acrylic acid)) with PAH were the polyelectrolytes of choice for this study because of their commercial relevance and widespread application in both academia and industry.[8,51−55] In this report, the acidic form of PAA and its sodium salt form are distinguished by different acronyms as PAA and PAANa, while the chloride salt of poly(allylamine) is referred to as PAH to maintain consistency with the previous literature.

Despite the extensive use of PAA (or PAANa) and PAH, the interplay between electrostatic and other noncovalent interactions on complexation between these two kinds of polymers remains unclear, resulting in inconsistencies among reports on their phase behaviors, complex morphologies, and stability against salt in varying environments. On the one hand, Chollakup et al. investigated the salt resistance and amount of PAANa−PAH complexes and reported the maximum complexation along with the maximum salt resistance (∼1−1.5 M) of complexes around pH = 7,[51,56] and Fu et al. ranked PAA as the weakest polyanion to complex with and the smallest ion-pairing strength among three other commonly used polyanions, and consequently, PAA-related complexes are expected to easily dissolve in the presence of an external salt.[57] On the other hand, several studies have reported that PAA-based complexes prepared under acidic conditions exhibit high salt resistances.[21,37,58] For example, Larson and co-workers pointed out that despite the pK_a of PAA being ∼5−5.5 and of PAH being ∼8.5−9.3,[59] the salt concentrations required to induce morphological transitions from precipitate to coacervate and from coacervate to solution were markedly asymmetric around pH 7 in PAA (and potassium salt of PAA)−PAH complexes, and critical KCl concentrations >3 M were required to completely dissolve the complexes; both these observations could not be explained solely by electrostatic interactions.[37] Lappan et al. reported significantly slower dynamics of PAA chains in complexes prepared under acidic conditions,[60] suggesting stronger association of the polymer network under low pH conditions. Thus, a comprehensive study of the phase behavior of PAA−PAH under various pH conditions is required to address the inconsistencies in PAA−PAH phase behavior. We address these inconsistencies by highlighting the role of hydrophobic interactions of the polyelectrolyte backbones and hydrogen bonding on the phase behavior and salt resistance of PAA−PAH complexes. The contributions from these nonelectrostatic interactions are shown to become especially prominent in high salt concentrations or under acidic conditions, wherein the electrostatic interactions are screened or weakened, respectively.

Mixing of PAANa and PAH (degree of polymerizations 158 and 160, respectively, Table S1) at equivalent monomer concentrations (to ensure charge matching), controlled total polymer concentration and added salt (NaCl) concentration, $C_{P,0}$ and $C_{S,added}$, respectively, led to complexation instantly. The mixture became turbid with flaky white precipitates[53,56]

https://dx.doi.org/10.1021/acs.macromol.0c00999
Macromolecules 2020, 53, 7835−7844

suspended in the solution (Figure S1). The first row in Figure 1 shows representative micrographs of the sedimented complexes with increasing concentration of added salt $C_{S,added}$ in PAANa−PAH complexes with total polymer concentration $C_{P,0}$ = 5% wt/v at pH = 6.5. Flaky PEC precipitates in the absence of added salt ($C_{S,added}$ = 0 M) transitioned to gel-like irregularly shaped droplets to liquid-like spherical PEC droplets with increasing $C_{S,added}$, indicative of increasing water content in the complexes. Interestingly, complexation persisted until $C_{S,added}$ = 4 M, in agreement with the values reported earlier by Perry et al.[61]

The salt concentration required to eliminate phase separation, referred to as the *salt resistance* (C_{SR}) of the complexes, is often obtained using turbidimetry.[11,17,56,62−67] Figure 2a shows a typical evolution of turbidity with increasing $C_{S,added}$ in PAANa−PAH complexes with $C_{P,0}$ = 5% wt/v at pH = 6.5. Turbidity of the solution decreased with increasing $C_{S,added}$ and was ascribed to diminishing differences between the refractive indices of the complex and the supernatant phases arising from the increasing water content in the complex phase[44,66,68,69] caused by a combination of stronger screening of electrostatic interactions among the oppositely charged chains and decreasing small ion entropy gains arising from complexation of the polyelectrolytes. Solution turbidity diminished and plateaued at C_{SR} = 2.0 M. A similar evolution of turbidity with $C_{S,added}$ for complexes with varying $C_{P,0}$ was observed (Figure S2). Vanishing turbidity, however, could not be definitively associated with complete dissolution of the complexes. At high $C_{S,added}$ values (≥2 M), the complexes sedimented to the bottom of the solutions, leading to clear supernatant phases. These precipitates were evident from a microscopic inspection of the solutions and are shown in Figure 1 and the inset in Figure 2a. These observations may explain the inconsistencies in the previously reported results from different studies which relied on turbidimetric analysis to identify phase separation.[37,51,56,57,61] Furthermore, we note that the complexes reported here and in earlier studies span a range of physical morphologies from liquid droplets to amorphous solids, which may lead to inconsistencies in the turbidity measurements. Therefore, as a guideline, combining turbidimetry with other visual characterization techniques such as optical microscopy is recommended to unambiguously identify phase transitions in PEC solutions. Furthermore, immediate measurements of turbidity after sample preparation are recommended to avoid inaccurate measurements of turbidity arising from flocculation.

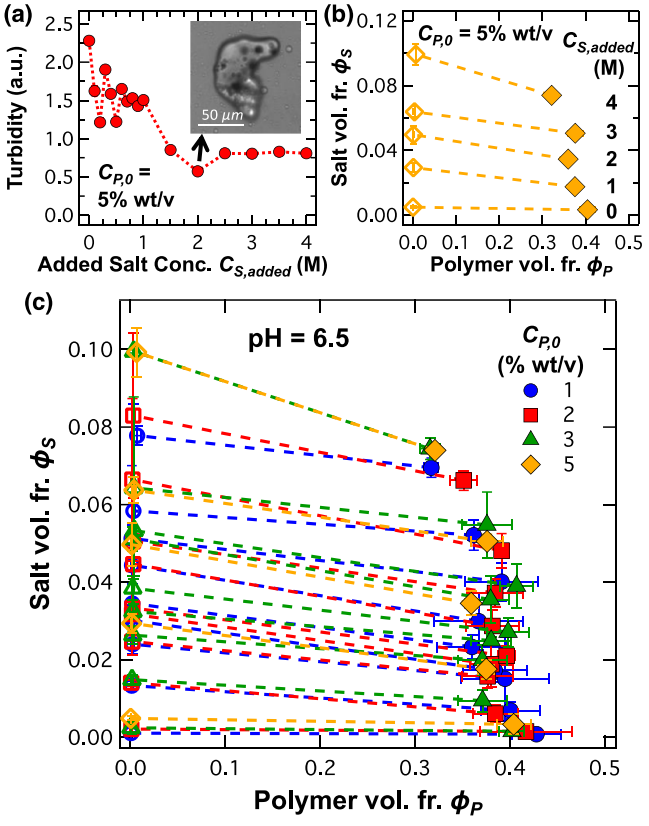

Figure 2. (a) Turbidity and (b) composition map depicting the total polymer and total salt content in the complex and supernatant phases of polymer-charge-matched mixtures comprising $PAANa_{158}$ (sodium salt), PAH_{160}, and NaCl prepared under neutral condition (pH = 6.5) at a total polymer concentration $C_{P,0}$ = 5% wt/v and added salt concentrations $C_{S,added}$ varying from 0 to 4 M. In (b), the filled (complex phase) and open (supernatant phase) symbols are connected by dotted coexistence lines. (c) Overlaid binodal phase boundaries of mixtures described in (b) prepared at total polymer concentration $C_{P,0}$ = 1, 2, 3, and 5% wt/v and added salt concentrations varying from 0 to 4 M. Data in (b,c) were obtained from TGA of the complex and the supernatant phases. Error bars in (b,c) denote the standard deviations in each measurement.

A quantification of PEC phase behavior was pursued through compositional analysis (water, polymer, and salt contents) of the complex and the supernatant phases using a thermogravimetric analysis (TGA) protocol developed in our previous report[69] (see the Supporting Information for experimental protocols). Figure 2b shows the binodal phase boundaries for PAANa−PAH complexes with $C_{P,0}$ = 5% wt/v under neutral conditions (pH = 6.5) mapped on the polymer concentration (ϕ_P)—salt concentration (ϕ_S) space. Pairs of points, connected by dashed lines, correspond to the compositions of the two phases resulting from bulk phase separation of complex and supernatant phases, represented by filled and unfilled symbols, respectively. The complex phase was found to have slightly smaller counterion concentration than the supernatant phase, as depicted by the negative slopes of the lines connecting the compositions of the two phases. This observation is contrary to V−O theory but in agreement with our previous experimental findings[69] and other recent experimental reports.[13,28,29,70]

Trends in binodal phase behaviors under neutral conditions were largely conserved for PECs with other $C_{P,0}$ values (=1, 2, and 3% wt/v, Figure S3). The polymer content of the complex phase ϕ_P generally decreased with increasing $C_{S,added}$, attributed to the screening of electrostatic interactions by the addition of salt, in accordance with the V−O theory[3] and previous studies.[20,26,44] Figure 2c (also see Figure S4) shows a good overlap of the binodal phase boundaries for PAANa−PAH complexes at pH = 6.5 with $C_{P,0}$ ranging from 1 to 5% wt/v and $C_{S,added}$ ranging from 0 to 4 M. In most cases, the salt ions were found to partition preferentially into the supernatant phases. This salt partitioning behavior can be surmised to be consistent irrespective of the hydrophobic or hydrophilic[3,5,28,69] nature of the backbone. It must be noted that preferential partitioning of salt into the complex phase may yet be imposed by molecular engineering of the polymer and counterion identities (different chemical structures, valency, and physical features).[70,71]

https://dx.doi.org/10.1021/acs.macromol.0c00999
Macromolecules 2020, 53, 7835−7844

Upon closer inspection, however, unique trends emerged in the binodal phase boundaries. The merging of the complex branch with the supernatant branch, an indication of the transition from the two-phase region into one homogeneous phase, was not observed even up to 4.0 M of added NaCl (Figure 2b), consistent with observation of complexes in microscopy experiments (Figure 1, first row). Furthermore, ϕ_P initially decreased with increasing $C_{S,added}$ in the range of $0 < C_{S,added} < 0.5$ M and then plateaued for $0.5 < C_{S,added} < 1.5$ M before decreasing again for $C_{S,added} > 1.5$ M. These behaviors are distinct from previous reports[13,21,72] on PEC phase behavior where ϕ_P monotonically and continuously decreased with increasing $C_{S,added}$ and can be tentatively ascribed to the increasing influence of nonelectrostatic intermolecular interactions on the complex phase behavior.

The morphology of PAANa−PAH complexes under basic conditions (pH = 9) exhibited an evolution with $C_{S,added}$ similar to the complexes under neutral conditions (second row in Figure 1). The binodal phase boundaries of PAANa−PAH complexes under basic conditions, obtained by superposing the composition data from PECs prepared with varying $C_{P,0}$, are summarized in Figure 3 (also see Figure S4). The composition

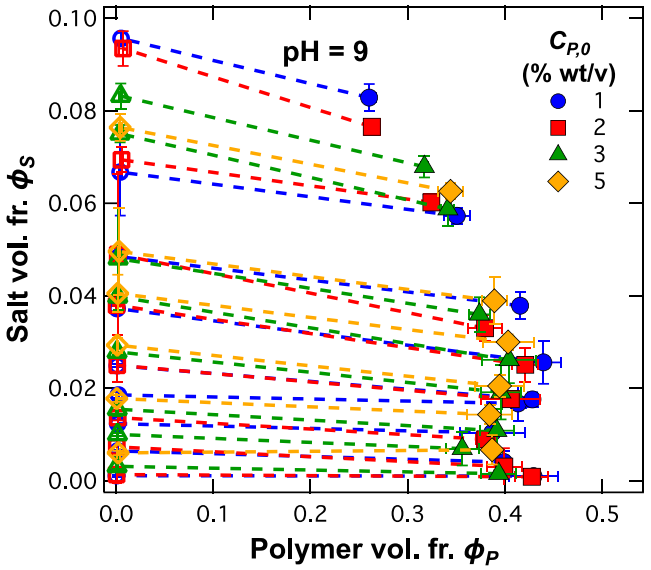

Figure 3. Overlaid binodal phase boundaries depicting the total polymer and total salt content in the complex and supernatant phases, obtained from TGA, of polymer-charge-matched mixtures comprising $PAANa_{158}$ (sodium salt), PAH_{160}, and NaCl prepared under basic condition (pH = 9) at total polymer concentrations $C_{P,0}$ = 1, 2, 3, and 5% wt/v and added salt concentrations varying from 0 to 4 M. The filled (complex phase) and open (supernatant phase) symbols are connected by dotted coexistence lines. Error bars denote the standard deviations in each measurement.

of the two phases and the shape of the phase envelope is similar to the map shown in Figure 2c (individual data sets for different $C_{P,0}$ are compiled in Figure S5). Furthermore, similar to complexes under neutral conditions, ϕ_P plateaued for PECs with $0.5 \text{ M} < C_{S,added} < 1.5$ M (Figure S5).

Because both PAANa and PAH are weak polyelectrolytes, their ionization is strongly affected by the pH of the environment. Under basic conditions, PAH ionized partially (24%, Figure S6), in effect reducing the charge density of the polyelectrolyte and propensity for complexation.[73] The similarity of the overall phase boundaries obtained under neutral and basic conditions, however, points toward the analogous role of electrostatic and other intermolecular interactions in dictating the PEC phase behavior under these conditions, with the partial ionization of PAH only contributing to diminish electrostatic correlations and increased water contents in the complexes. Furthermore, we hypothesize that cooperativity of electrostatic interactions between cationic and anionic chains promotes the ionization of PAH chains under basic conditions, leading to the similarity of the binodal phase boundaries under basic and neutral conditions.[74,75] We expect these observations to inspire theoretical and simulation investigations that in turn will provide further insights into the phenomena.

The morphology of PECs comprising the acidic form of PAA (degree of polymerization 138, Table S1) with PAH prepared under acidic conditions (pH = 3), however, was remarkably different from those obtained under basic and neutral conditions (third row in Figure 1). This adjustment of the polyanion was required because PAANa was found to precipitate when it was rendered un-ionized and neutral in pH = 3 solutions. At the same time, we acknowledge that using the acidic form of PAA and volatility of HCl formed from counterions during the TGA analysis may contribute to minor differences between the measured and actual ϕ_S values. In contrast to the continuous evolution of complex morphology with increasing $C_{S,added}$ under neutral and basic conditions, the complexes prepared under acidic conditions were found to retain their flaky precipitate morphology even at the highest $C_{S,added}$ investigated (third row in Figure 1).

Binodal phase boundaries of complexes prepared under acidic conditions were also remarkably different from those obtained under basic and neutral conditions, particularly in the low ϕ_S region. Notably, complexes formed under low pH, rather than round-shaped coacervate droplets, were observed to be precipitates, which might be in the kinetically trapped state within the time frame of the conducted experiment. Figure 4a exemplifies the distinctive phase diagram for $C_{P,0}$ = 3% wt/v; Figure 4b presents the superimposed phase diagrams at $C_{P,0}$ = 1, 2, 3, and 5% wt/v with $C_{S,added}$ ranging from 0 to 4 M (individual data sets for different $C_{P,0}$ are compiled in Figure S7, also see Figure S4). Specifically, the complex branch extended right toward higher ϕ_P with increasing $C_{S,added}$ until $C_{S,added} < 1$ M, which indicated enriching of the polyelectrolyte content in the complex phase with addition of salt, opposite of the trends from the other two conditions. For $C_{S,added} > 1$ M, the trends of decreasing ϕ_P with increasing $C_{S,added}$ were recovered. This unusual trend of increasing polymer content in the complex phase upon increasing salt concentration in the solution was consistent regardless of the $C_{P,0}$ values. Furthermore, the phase separation was found to be $C_{P,0}$-dependent, as evident from the significant differences in the complex compositions at high $C_{S,added}$ and from the intersecting coexistence lines (denoted by dashed lines in Figure 4b). This is in contrast to the $C_{P,0}$-independent phase behavior with nonintersecting phase coexistence lines in neutral and basic PECs, as shown in Figures 2c and 3.

The complexes were found to be asymmetric in concentration of PAA and PAH under acidic conditions, ascribable to partial ionization of PAA chains under the acidic conditions. ^{1}H NMR spectra of the complexes prepared at $C_{P,0}$ = 3% wt/v and $C_{S,added}$ = 2.0 M indeed showed that the molar ratio of PAA to PAH was 0.67 in complexes prepared under acidic conditions, as compared to 0.43 and 0.40 in their counterparts

https://dx.doi.org/10.1021/acs.macromol.0c00999
Macromolecules 2020, 53, 7835−7844

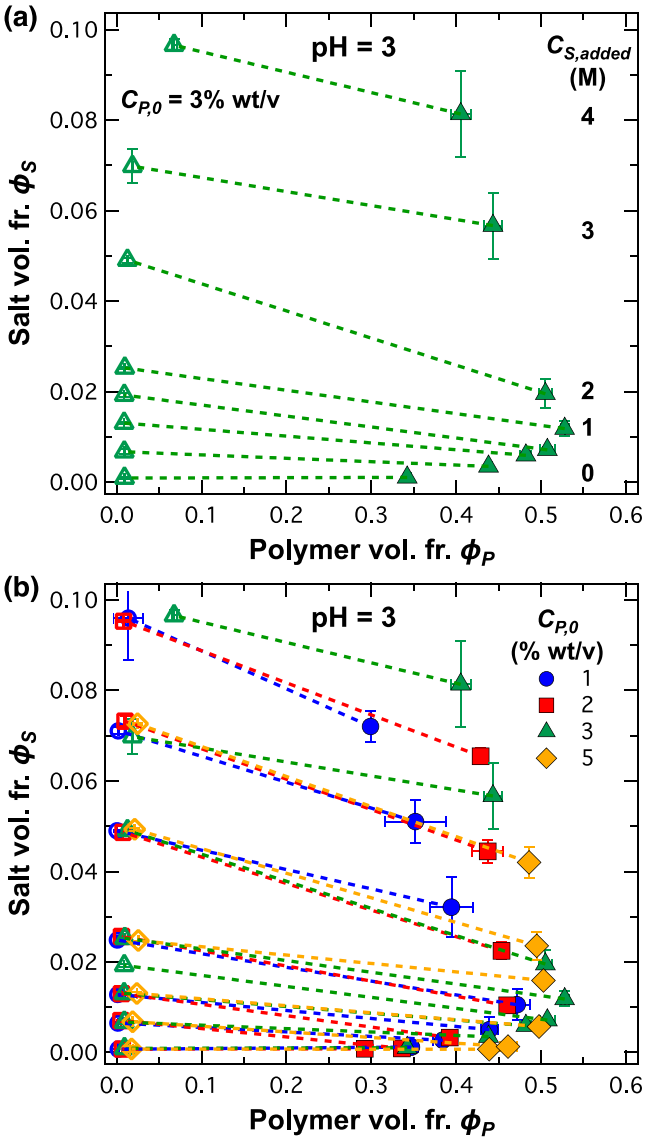

Figure 4. (a) Composition map depicting the total polymer and total salt content in the complex and supernatant phases, obtained from TGA, of polymer-charge-matched mixtures comprising PAA_{138}, PAH_{160}, and NaCl prepared under acidic condition (pH = 3) at a total polymer concentration $C_{P,0}$ = 3% wt/v and added salt concentrations varying being 0, 0.25, 0.5, 0.75, 1, 2, 3, and 4 M from bottom to top. The filled (complex phase) and open (supernatant phase) symbols are connected by dotted coexistence lines. (b) Overlaid binodal phase boundaries of mixtures described in (b) prepared at total polymer concentrations $C_{P,0}$ = 1, 2, 3, and 5% wt/v and added salt concentrations varying from 0 to 4 M. Error bars in (a,b) denote the standard deviations in each measurement.

prepared under neutral and basic conditions, respectively (Figure S8, Table S3), in good agreement with the previous literature.[8,37] Under neutral and basic conditions, the deviations from equimolar PEC compositons can be attributed to the commercial synthesis of the polymers employed in this study, leading to partial functionalization of the PAA and PAH backbones. At the same time, a combination of associative phase separation of PAA and PAH as well as segregative phase separation of PAA could thus be argued to result in the formation of complexes under acidic conditions.

These unique trends in the composition maps appear similar to the salting-in and salting-out behavior of polyelectrolytes (with strong electrostatic interactions) that can occur upon increasing concentration of monovalent and multivalent salts, as has been suggested by Zhang et al.[30] In polyelectrolyte solutions, this behavior was proposed to arise from an interplay between increasing translational entropy of salt ions and excluded volume interactions promoting homogenization of the solution competing with electrostatic correlations favoring phase separation. In PEC systems, salting out is typically not observed owing to small translational entropy of the oppositely charged polyelectrolyte chains dominated by the strong electrostatic correlations between them. With increasing salt concentrations, however, a salting-in phenomenon is consistently observed.[5] In PAA−PAH complexes under acidic conditions, however, PAA is expected to partially ionize (3%, Figure S6), resulting in weak electrostatic correlations between the PAA and PAH chains. Electrostatic correlations between the oppositely charged chains, mediated by monovalent counterions, are expected to increase initially with increasing $C_{S,added}$, leading to increasing ϕ_P in the PECs. At higher $C_{S,added}$, counterion entropy and excluded volume interactions eventually dominate the phase behavior, resulting in decreasing ϕ_P in the PECs. We note that salting-in and salting-out phenomena have been described in the literature for four-component systems (polyelectrolytes, salt ions, and water) while the system considered here is a five-component system comprising two polyelectrolytes, limiting the conclusion that could be drawn from the theoretical descriptions of the former for the latter systems.

In addition to lower ionization of the PAA (3%, Figure S6) chains leading to weaker electrostatic correlations, hydrophobic interactions of the hydrocarbon backbone of the partially ionized PAA chains with water and the hydrogen bonding of acrylic acid moieties are also expected to influence the PEC phase behavior.[76,77] The un-ionized functional groups in PAA can serve as hydrogen-bond donors and/or acceptors; Buscall and Corner proposed that hydrogen bonding can be facilitated under acidic conditions for PAA.[77] Upon addition of salt, both hydration and hydrogen bonding are disrupted, owing to screening of electrostatic interactions by the salt ions and the reduced availability of water molecules to form hydrogen bonds. Phase separation of the PAA from water may occur in such a case upon the formation of intra- and interchain hydrogen bonds among the ionized acrylic acid moieties, accompanied by the unfavorable interactions of the aliphatic backbone with water.

The influence of salt on solubility of individual polyelectrolytes, PAA and PAH, in water was investigated using turbidimetric analysis and optical microscopy. Although PAH solutions remained stable across the pH range investigated, PAA was found to phase-separate even at salt concentrations as low as 0.15 M. Figure 5a shows the turbidity of 5% wt/v PAA and 5% wt/v PAH solutions as a function of salt concentration. Although the PAH solutions remained clear upon addition of salt, the absorbance of the PAA solution steadily increased beginning at 0.15 M NaCl concentrations, indicating phase separation of PAA. Aggregates could also be identified upon visual and microscopic inspection. At salt concentration >0.5 M, PAA precipitates began to agglomerate and sediment at the bottom of the solution, leading to lower turbidity. Eventually, turbidity returned to the baseline following complete sedimentation of PAA agglomerates. The inset in Figure 5a

https://dx.doi.org/10.1021/acs.macromol.0c00999
Macromolecules 2020, 53, 7835−7844

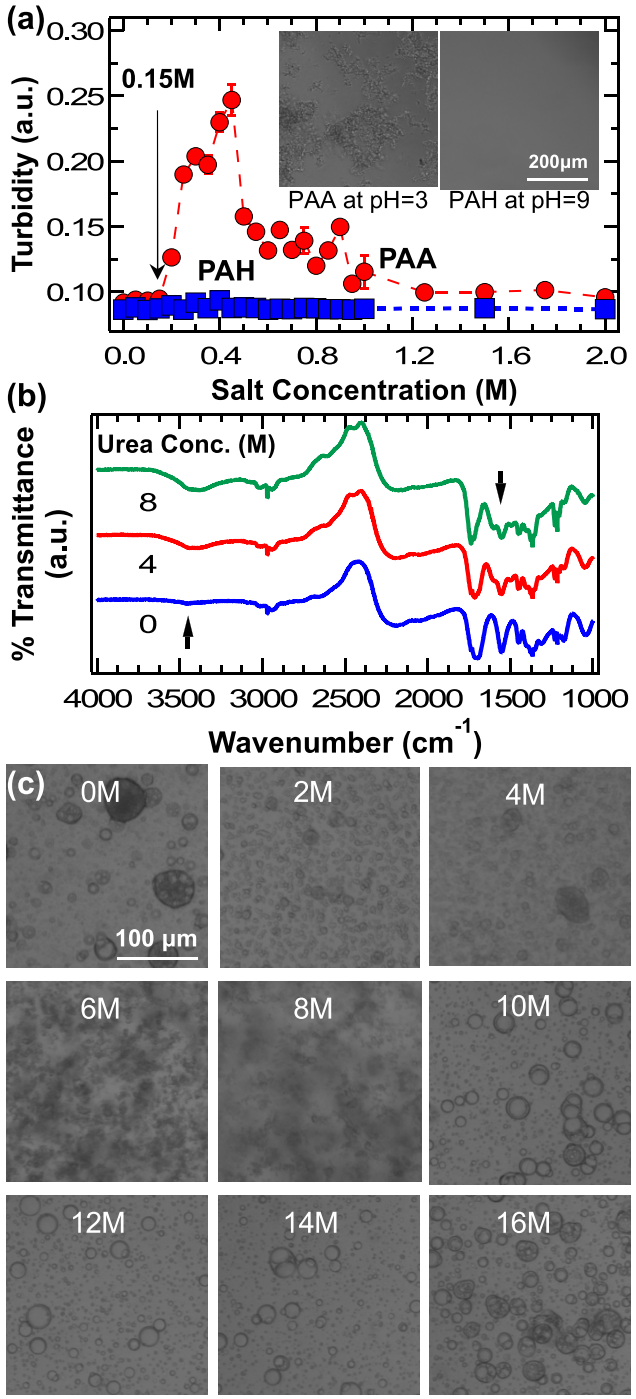

Figure 5. (a) Turbidity of aqueous PAA and PAH solutions (1% wt/v) with increasing salt concentration. Increasing turbidity upon addition of salt >0.15 M corresponded to PAA precipitation. Subsequent decrease in turbidity at higher salt concentrations resulted from sedimentation of the PAA precipitates. *Insets* depict representative micrographs of 5% wt/v PAA (pH = 3) and PAH (pH = 9) solutions with 2 M NaCl. The scale bars were the same for both images. (b) FTIR spectra of PAA−PAH PECs prepared in pH = 3 solutions with 0, 4, and 8 M of urea. Arrows at ∼3450 and ∼1560 cm^{-1} indicate free O−H stretching vibrations and hydrogen bonding of the deprotonated carboxylic acids, respectively. (c) Micrographs of the complexes with $C_{P,0}$ = 1% wt/v, $C_{S,added}$ = 2 M, and pH = 3 and urea concentration ranging from 0 to 16 M. The scale bars are the same for all images.

shows a representative microscopic image of 5% wt/v PAA solution at pH = 3 with 2.0 M NaCl with considerable precipitation. Increasing ϕ_P in the complex phase with increasing $\phi_{S,added}$ for $\phi_{S,added}$ < 1 M and the asymmetry in the polymer content in the complexes can thus be attributed partially to this precipitation of PAA in saline solutions. Again, we note that the behavior of the PAA chain in salt solutions may be different from the PAA−PAH solutions owing to strong electrostatic interactions, cooperative polyelectrolyte ionization, and diminished role of counterion entropy in dictating stability of the complexed polyelectrolyte chains in the PEC systems.

At the same time, the effect of hydrogen bonding on PEC phase behavior under acidic conditions was examined by preparing PECs in deuterium oxide (D_2O) with increasing concentrations of urea to progressively inhibit hydrogen bonding in the system. Fourier transform infrared (FTIR) spectra of PAA−PAH complexes with 0, 4, and 8 M urea, shown in Figure 5b (also see Figure S9), show clear evidence of weakened intermolecular or intramolecular hydrogen bonding between PAA chains. Specifically, band sharpening at ∼3450 cm^{-1} corresponds to increasing O−H stretching as urea concentration increased and broadening of a sharp single peak at ∼1560 cm^{-1} into a bimodal peak corresponds to urea forming hydrogen bonds with deprotonated −COOH moieties. These results indicate disruption of hydrogen bonding among PAA chains upon addition of urea.

The morphology of the PECs also varied distinctively with increasing urea concentrations. Figure 5c displays a representative collection of micrographs for the PAA−PAH complexes prepared at $C_{P,0}$ = 1% wt/v, $C_{S,added}$ = 2.0 M, and pH = 3 with increasing urea concentration from 0 to 16 M (the maximum achievable concentration of urea at 20 °C). PEC morphology changed from viscous gel to flaky precipitates and finally to spherical agglomerates. Correspondingly, the weight fraction of water in the PECs, measured by TGA, increased from 41.39 to 57.95% (Table S2). Thus, it could be surmised that urea influenced the intermolecular interactions between the oppositely charged chains and PEC phase behavior in a nontrivial manner by weakening the hydrogen-bonded acrylic networks. At the same time, the close association of the primary amine group of PAH with the carboxyl group on PAA also contributes to the high salt resistance as indicated by Fu et al.[57] However, because the complexes persisted and exhibited reasonably high salt tolerance under exceptionally high urea contents wherein hydrogen bonding is diminished, it could be argued that while hydrogen bonding may be dictating the morphology of the PECs and also promoting precipitation of PAA upon addition of salt, it could not be contributing toward the unusual high salt tolerance of PAA−PAH PECs.

Larson and co-workers reported similar experimental observations of unusually high, pH-asymmetric salt resistance of the PECs comprising PAA (and potassium salt of PAA) and poly(*N*,*N*-dimethylaminoethyl methacrylate) (PDMAEMA).[37] Atomistic simulations showed unionized and charged acrylic acid moieties forming 2.5 and 6 hydrogen bonds with water, highlighting the hydrophobic nature of the unionized acrylic acid.[37] At the same time, both neutral and charged PDMAEMA monomers formed two hydrogen bonds with water, emphasizing the role of PAA in influencing the phase behavior of the PAA−PDMAEMA system. We expect similar factors to influence the phase behavior and salt resistance of PAA−PAH PECs.

https://dx.doi.org/10.1021/acs.macromol.0c00999
Macromolecules 2020, 53, 7835−7844

The effect of backbone hydrophobicity and hydrogen bonding and the influence of salt on polyelectrolyte−solvent interactions can be described by an effective interaction parameter, χ_{eff} as $\chi_{eff} = \chi_0 - w_c/\kappa^2$, where w_c is the strength of the screened Coulombic interaction among monomers, κ^2 is the inverse-square Debye screening length, proportional to salt concentration, and χ_0 is the intrinsic interaction parameters.[4,78] χ_{eff} = 0.5 has been reported for PAA in salt-free aqueous solutions.[79,80] Increasing salt concentration increases κ^2, leading to a χ_{eff} > 0.5 signifying unfavorable interactions between PAA and water in saline solutions. Unsurprisingly, a quantitative prediction of the pH-asymmetric salt resistance of PAA−PDMAEMA PECs was obtained by including a Flory−Huggins interaction parameter χ = 0.75 representing the interactions between PAA and water into the classic V−O model for PEC phase behavior.[37] Moreover, the polymer volume fraction of PAA(PAANa)−PAH complexes investigated in this study was remarkably higher than those observed in polypeptide PECs,[69] which is in agreement with earlier RPA-based predictions.[25,26] Importantly, Kudlay and Olvera de la Cruz also identified small decrease followed by an increase in the polymer volume fraction in the complex phase as a function of salt concentration for χ values near and above 0.5, qualitatively similar with the trend shown in Figure 4.[25]

PEC phase behavior under different pH conditions was compared in Figure 6 showing the polymer−salt compositions for PECs prepared at (a) $C_{P,0}$ = 1% wt/v and (b) $C_{P,0}$ = 5% wt/v. Although the compositions of PECs starting with $C_{P,0}$ = 1% wt/v obtained at pH = 3, 6.5, and 9 were similar, the trends with increasing $C_{S,added}$ were divergent (Figure 6a). The divergence increased in the PECs starting with $C_{P,0}$ = 5% wt/v (Figure 6b), which can be ascribed to stronger hydrophobicity and hydrogen bonding effects accompanying higher polymer concentrations and the nonequilibrium effects that may emerge from increasing kinetic arrest of complexes at higher polymer concentrations. These effects also limited the accessible limits of salt additions, wherein the highest $C_{S,added}$ in 5% wt/v samples was 2.5 M compared to 4.0 M for 1% wt/v samples.

In summary, the compositions of the PECs prepared under basic and neutral conditions were similar. The general trends, including screening effect of salt, decreasing polymer content in the complex phase for PECs prepared at higher total polymer concentration (termed as self-suppression), and preferential partitioning of counterions, were also similar in the two cases. Under neutral conditions, both polymers were fully ionized. Under basic conditions, although PAH was partially ionized (PAANa was completely ionized), the complexation behavior was not significantly affected. The association of ionized amino groups in PAH with carboxyl groups in PAA, facilitated by hydroxide ions in the aqueous solutions, is expected to result in the formation of stable complexes and drive the cooperative ionization of PAH chains. However, PECs prepared under acidic conditions showed an entirely different behavior. Under these conditions, the PAA chains were partially ionized and a fraction of the polyelectrolyte chains precipitated under high salt conditions, rendering them unable to complex associatively with PAH chains. The solid precipitates formed under low pH conditions comprised both pure PAA precipitates (with phase separation dominated by backbone hydrophobicity and hydrogen bonding) and PAA−PAH complexes, which led to higher PAA content in precipitates and an increase in the polymer content in the precipitates upon addition of salt. The unusual

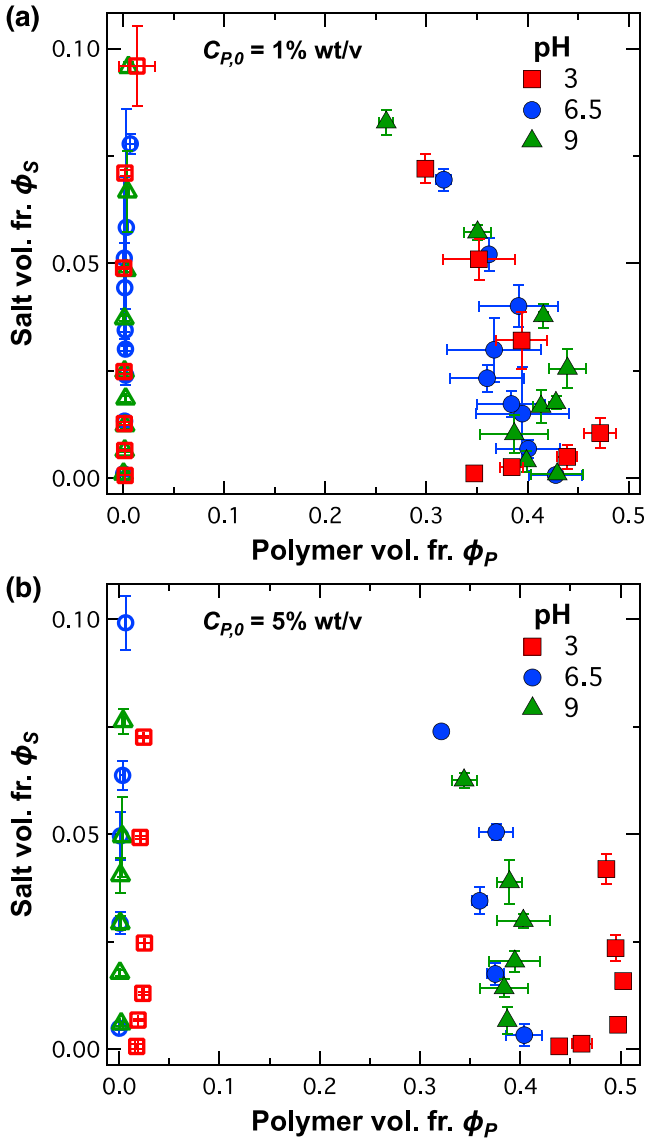

Figure 6. Comparison of the binodal phase boundaries for PAA(PAANa)−PAH complexes prepared under three different pH conditions with $C_{P,0}$ = (a) 1% wt/v and (b) 5% wt/v. Although large portions of the phase boundaries under neutral and basic conditions overlap, the phase boundaries under acidic conditions exhibit nontrivial deviations owing to the influence of hydrophobic interactions and hydrogen bonding on the phase behavior of the complexes.

PAA accumulation in the phase-separated complexes under acidic conditions can therefore be surmised to occur with associative and segregative phase separation working simultaneously. In this sense, the phase behavior of the PAA and PAH system, instead of being understood as simple polyelectrolyte complexation, can be regarded to emerge from a combined action of various intermolecular interaction, including electrostatics, hydrophobicity, and hydrogen bonding. The experimentally measured compositional maps reflect the superimposed result of these intermolecular interactions as a function of polymer concentration, salt concentration, and pH.

Altogether, this investigation brought attention to the fact that the complexation of oppositely charged polyelectrolytes is a fairly complicated phenomenon driven by not only electrostatic forces and entropic gains from counterion

https://dx.doi.org/10.1021/acs.macromol.0c00999
Macromolecules 2020, 53, 7835−7844

release[81,82] but also solvent effect and unavoidable intermolecular interactions. The nature of the phase separation process may change from electrostatic associative complexation to solvent-effect-driven segregative precipitation. Oftentimes, such factors in realistic materials such as PAA and PAH are overlooked or assumed to be inconsequential compared to charge-driven complexation mechanisms. To incorporate more of these advanced features into a wider material infrastructure, we anticipate that theory and simulations can more easily interrogate the interplay of such variables. This experimental work elucidated molecular level insight of various complexation effects for the model polymer pairing of PAA(Na) and PAH, which can enable greater comprehension and control over the structure−property relationship of synthetic polymeric systems in micellar and gel-like architectures.[83−85]

■ ASSOCIATED CONTENT

Supporting Information

The Supporting Information is available free of charge at https://pubs.acs.org/doi/10.1021/acs.macromol.0c00999.

Materials and methods, supplementary figures, and supplementary tables (PDF)

■ AUTHOR INFORMATION

Corresponding Authors

Samanvaya Srivastava − *Chemical and Biomolecular Engineering, University of California, Los Angeles, Los Angeles, California 90095, United States;* orcid.org/0000-0002-3519-7224; Email: samsri@ucla.edu

Matthew V. Tirrell − *Pritzker School of Molecular Engineering, The University of Chicago, Chicago, Illinois 60637, United States; Center for Molecular Engineering and Materials Science Division, Argonne National Laboratory, Lemont, Illinois 60439, United States;* Email: mtirrell@uchicago.edu

Authors

Lu Li − *Pritzker School of Molecular Engineering, The University of Chicago, Chicago, Illinois 60637, United States*

Siqi Meng − *Pritzker School of Molecular Engineering, The University of Chicago, Chicago, Illinois 60637, United States;* orcid.org/0000-0002-2238-9278

Jeffrey M. Ting − *Pritzker School of Molecular Engineering, The University of Chicago, Chicago, Illinois 60637, United States;* orcid.org/0000-0001-7816-3326

Complete contact information is available at: https://pubs.acs.org/10.1021/acs.macromol.0c00999

Author Contributions

S.S. and M.V.T. conceptualized the study. S.S. and L.L. designed the experiments. L.L. performed the experiments with help from S.M. L.L., S.S., J.M.T., and M.V.T. contributed to the analysis/interpretation of the data and wrote the manuscript. S.S. and M.V.T. supervised the experimental work.

Funding

This work was performed under the following financial assistance award 70NANB19H005 from the U.S. Department of Commerce, National Institute of Standards and Technology (NIST) as part of the Center for Hierarchical Materials Design (CHiMaD), and MRSEC grant DMR-1420709 from the U.S. National Science Foundation. J.M.T. acknowledges financial support from the NIST-CHiMaD Postdoctoral Fellowship.

Notes

The authors declare no competing financial interest.

■ ACKNOWLEDGMENTS

The authors acknowledge Dr. Kazi Sadman for helpful discussions. We also acknowledge the support from Dr. J. Juller from the James Franck Institute at the University of Chicago during TGA.

■ REFERENCES

(1) de Jong, B.; Kruyt, H. G.; R, H. Koazervation. *Proc. K. Ned. Akad. Wet.* **1929**, *32*, 849−856.

(2) Voorn, M. J.*Complex Coacervation*; Wiley-VCH Verlag GmbH Co.: Amsterdam, 1956.

(3) Overbeek, J. T. G.; Voorn, M. J. Phase Separation in Polyelectrolyte Solutions. Theory of Complex Coacervation. *J. Cell. Comp. Physiol.* **1957**, *49*, 7−26.

(4) Muthukumar, M. 50th Anniversary Perspective : A Perspective on Polyelectrolyte Solutions. *Macromolecules* **2017**, *50*, 9528−9560.

(5) Srivastava, S.; Tirrell, M. V. Polyelectrolyte Complexation. *Adv. Chem. Phys.* **2016**, *161*, 499−544.

(6) Brangwynne, C. P.; Tompa, P.; Pappu, R. V. Polymer Physics of Intracellular Phase Transitions. *Nat. Phys.* **2015**, *11*, 899−904.

(7) Strom, A. R.; Emelyanov, A. V.; Mir, M.; Fyodorov, D. V.; Darzacq, X.; Karpen, G. H. Phase Separation Drives Heterochromatin Domain Formation. *Nature* **2017**, *547*, 241−245.

(8) Wang, Q.; Schlenoff, J. B. Single- and Multicompartment Hollow Polyelectrolyte Complex Microcapsules by One-Step Spraying. *Adv. Mater.* **2015**, *27*, 2077−2082.

(9) Srivastava, S.; Andreev, M.; Levi, A. E.; Goldfeld, D. J.; Mao, J.; Heller, W. T.; Prabhu, V. M.; De Pablo, J. J.; Tirrell, M. V. Gel Phase Formation in Dilute Triblock Copolyelectrolyte Complexes. *Nat. Commun.* **2017**, *8*, 14131.

(10) Aumiller, W. M.; Pir Cakmak, F.; Davis, B. W.; Keating, C. D. RNA-Based Coacervates as a Model for Membraneless Organelles: Formation, Properties, and Interfacial Liposome Assembly. *Nat. Chem.* **2016**, *32*, 10042−10053.

(11) Aumiller, W. M.; Keating, C. D. Phosphorylation-Mediated RNA/Peptide Complex Coacervation as a Model for Intracellular Liquid Organelles. *Nat. Chem.* **2016**, *8*, 129−137.

(12) Meng, X.; Schiffman, J. D.; Perry, S. L. Electrospinning Cargo-Containing Polyelectrolyte Complex Fibers: Correlating Molecular Interactions to Complex Coacervate Phase Behavior and Fiber Formation. *Macromolecules* **2018**, *51*, 8821−8832.

(13) Meng, X.; Perry, S. L.; Schiffman, J. D. Complex Coacervation: Chemically Stable Fibers Electrospun from Aqueous Polyelectrolyte Solutions. *ACS Macro Lett.* **2017**, *6*, 505−511.

(14) Kuo, C.-H.; Leon, L.; Chung, E. J.; Huang, R.-T.; Sontag, T. J.; Reardon, C. A.; Getz, G. S.; Tirrell, M.; Fang, Y. Inhibition of Atherosclerosis-Promoting MicroRNAs via Targeted Polyelectrolyte Complex Micelles. *J. Mater. Chem. B* **2014**, *2*, 8142−8153.

(15) Black, K. A.; Priftis, D.; Perry, S. L.; Yip, J.; Byun, W. Y.; Tirrell, M. Protein Encapsulation via Polypeptide Complex Coacervation. *ACS Macro Lett.* **2014**, *3*, 1088−1091.

(16) Krogstad, D. V.; Lynd, N. A.; Miyajima, D.; Gopez, J.; Hawker, C. J.; Kramer, E. J.; Tirrell, M. V. Structural Evolution of Polyelectrolyte Complex Core Micelles and Ordered-Phase Bulk Materials. *Macromolecules* **2014**, *47*, 8026−8032.

(17) Priftis, D.; Tirrell, M. Phase Behaviour and Complex Coacervation of Aqueous Polypeptide Solutions. *Soft Matter* **2012**, *8*, 9396−9405.

(18) Fares, H. M.; Schlenoff, J. B. Diffusion of Sites versus Polymers in Polyelectrolyte Complexes and Multilayers. *J. Am. Chem. Soc.* **2017**, *139*, 14656−14667.

(19) Gucht, J. v. d.; Spruijt, E.; Lemmers, M.; Cohen Stuart, M. A. Polyelectrolyte Complexes: Bulk Phases and Colloidal Systems. *J. Colloid Interface Sci.* **2011**, *361*, 407−422.

(20) Veis, A.; Bodor, E.; Mussell, S. Molecular Weight Fractionation and the Self-suppression of Complex Coacervation. *Biopolymers* **1967**, *5*, 37−59.
(21) Salehi, A.; Desai, P. S.; Li, J.; Steele, C. A.; Larson, R. G. Relationship between Polyelectrolyte Bulk Complexation and Kinetics of Their Layer-by-Layer Assembly. *Macromolecules* **2015**, *48*, 400−409.
(22) Bucur, C. B.; Sui, Z.; Schlenoff, J. B. Ideal Mixing in Polyelectrolyte Complexes and Multilayers: Entropy Driven Assembly. *J. Am. Chem. Soc.* **2006**, *128*, 13690−13691.
(23) Fu, J.; Schlenoff, J. B. Driving Forces for Oppositely Charged Polyion Association in Aqueous Solutions: Enthalpic, Entropic, but Not Electrostatic. *J. Am. Chem. Soc.* **2016**, *138*, 980−990.
(24) Qin, J.; De Pablo, J. J. Criticality and Connectivity in Macromolecular Charge Complexation. *Macromolecules* **2016**, *49*, 8789−8800.
(25) Kudlay, A.; Olvera de la Cruz, M. Precipitation of Oppositely Charged Polyelectrolytes in Salt Solutions. *J. Chem. Phys.* **2004**, *120*, 404−412.
(26) Kudlay, A.; Ermoshkin, A. V.; Olvera de la Cruz, M. Complexation of Oppositely Charged Polyelectrolytes: Effect of Ion Pair Formation. *Macromolecules* **2004**, *37*, 9231−9241.
(27) Perry, S. L.; Sing, C. E. PRISM-Based Theory of Complex Coacervation: Excluded Volume versus Chain Correlation. *Macromolecules* **2015**, *48*, 5040−5053.
(28) Radhakrishna, M.; Basu, K.; Liu, Y.; Shamsi, R.; Perry, S. L.; Sing, C. E. Molecular Connectivity and Correlation Effects on Polymer Coacervation. *Macromolecules* **2017**, *50*, 3030−3037.
(29) Chang, L.-W.; Lytle, T. K.; Radhakrishna, M.; Madinya, J. J.; Vélez, J.; Sing, C. E.; Perry, S. L. Sequence and Entropy-Based Control of Complex Coacervates. *Nat. Commun.* **2017**, *8*, 1273.
(30) Zhang, P.; Alsaifi, N. M.; Wu, J.; Wang, Z.-G. Salting-Out and Salting-In of Polyelectrolyte Solutions: A Liquid-State Theory Study. *Macromolecules* **2016**, *49*, 9720−9730.
(31) Peng, B.; Muthukumar, M. Modeling Competitive Substitution in a Polyelectrolyte Complex. *J. Chem. Phys.* **2015**, *143*, 243133.
(32) Castelnovo, M.; Joanny, J.-F. Complexation between Oppositely Charged Polyelectrolytes: Beyond the Random Phase Approximation. *Eur. Phys. J. E* **2001**, *6*, 337−386.
(33) Priftis, D.; Laugel, N.; Tirrell, M. Thermodynamic Characterization of Polypeptide Complex Coacervation. *Langmuir* **2012**, *28*, 15947−15957.
(34) Vitorazi, L.; Ould-Moussa, N.; Sekar, S.; Fresnais, J.; Loh, W.; Chapel, J.-P.; Berret, J.-F. Evidence of a Two-Step Process and Pathway Dependency in the Thermodynamics of Poly(Diallyldimethylammonium Chloride)/Poly(Sodium Acrylate) Complexation. *Soft Matter* **2014**, *10*, 9496−9505.
(35) Wu, H.; Ting, J. M.; Werba, O.; Meng, S.; Tirrell, M. V. Non-Equilibrium Phenomena and Kinetic Pathways in Self-Assembled Polyelectrolyte Complexes. *J. Chem. Phys.* **2018**, *149*, 163330.
(36) Takahashi, R.; Narayanan, T.; Sato, T. Growth Kinetics of Polyelectrolyte Complexes Formed from Oppositely-Charged Homopolymers Studied by Time-Resolved Ultra-Small-Angle X-Ray Scattering. *J. Phys. Chem. Lett.* **2017**, *8*, 737−741.
(37) Jha, P.; Desai, P.; Li, J.; Larson, R. PH and Salt Effects on the Associative Phase Separation of Oppositely Charged Polyelectrolytes. *Polymers* **2014**, *6*, 1414−1436.
(38) Rumyantsev, A. M.; Zhulina, E. B.; Borisov, O. V. Complex Coacervate of Weakly Charged Polyelectrolytes: Diagram of States. *Macromolecules* **2018**, *51*, 3788−3801.
(39) Sato, H.; Nakajima, A. Complex Coacervation in Sulfated Polyvinyl Alcohol- Aminoacetalyzed Polyvinyl Alcohol System - II. Formation of Coacervate Droplets. *Colloid Polym. Sci.* **1974**, *252*, 944−948.
(40) Sato, H.; Nakajima, A. Complex Coacervation in Sulfated Polyvinyl Alcohol- Aminoacetalyzed Polyvinyl Alcohol System - I. Conditions for Complex Coacervation. *Colloid Polym. Sci.* **1974**, *252*, 294−297.
(41) Friedowitz, S.; Salehi, A.; Larson, R. G.; Qin, J. Role of Electrostatic Correlations in Polyelectrolyte Charge Association. *J. Chem. Phys.* **2018**, *149*, 163335.
(42) Salehi, A.; Larson, R. G. A Molecular Thermodynamic Model of Complexation in Mixtures of Oppositely Charged Polyelectrolytes with Explicit Account of Charge Association/Dissociation. *Macromolecules* **2016**, *49*, 9706−9719.
(43) Sadman, K.; Wang, Q.; Chen, Y.; Keshavarz, B.; Jiang, Z.; Shull, K. R. Influence of Hydrophobicity on Polyelectrolyte Complexation. *Macromolecules* **2017**, *50*, 9417−9426.
(44) Spruijt, E.; Westphal, A. H.; Borst, J. W.; Cohen Stuart, M. A.; Van Der Gucht, J. Binodal Compositions of Polyelectrolyte Complexes. *Macromolecules* **2010**, *43*, 6476−6484.
(45) Sun, J.; Perry, S. L.; Schiffman, J. D. Electrospinning Nanofibers from Chitosan/Hyaluronic Acid Complex Coacervates. *Biomacromolecules* **2019**, *20*, 4191−4198.
(46) Tabandeh, S.; Leon, L. Engineering Peptide-Based Polyelectrolyte Complexes with Increased Hydrophobicity. *Molecules* **2019**, *24*, 868.
(47) Lou, J.; Friedowitz, S.; Qin, J.; Xia, Y. Tunable Coacervation of Well-Defined Homologous Polyanions and Polycations by Local Polarity. *ACS Cent. Sci.* **2019**, *5*, 549−557.
(48) Huang, J.; Morin, F. J.; Laaser, J. E. Charge-Density-Dominated Phase Behavior and Viscoelasticity of Polyelectrolyte Complex Coacervates. *Macromolecules* **2019**, *52*, 4957−4967.
(49) Ali, S.; Bleuel, M.; Prabhu, V. M. Lower Critical Solution Temperature in Polyelectrolyte Complex Coacervates. *ACS Macro Lett.* **2019**, *8*, 289−293.
(50) Adhikari, S.; Prabhu, V. M.; Muthukumar, M. Lower Critical Solution Temperature Behavior in Polyelectrolyte Complex Coacervates. *Macromolecules* **2019**, *52*, 6998−7004.
(51) Chollakup, R.; Beck, J. B.; Dirnberger, K.; Tirrell, M.; Eisenbach, C. D. Polyelectrolyte Molecular Weight and Salt Effects on the Phase Behavior and Coacervation of Aqueous Solutions of Poly(Acrylic Acid) Sodium Salt and Poly(Allylamine) Hydrochloride Hydrochloride. *Macromolecules* **2013**, *46*, 2376−2390.
(52) Boas, M.; Burman, M.; Yarin, A. L.; Zussman, E. Electrically-Responsive Deformation of Polyelectrolyte Complex (PEC) Fibrous Membrane. *Polymer* **2018**, *158*, 262−269.
(53) Zhang, Y.; Li, F.; Valenzuela, L. D.; Sammalkorpi, M.; Lutkenhaus, J. L. Effect of Water on the Thermal Transition Observed in Poly(Allylamine Hydrochloride)-Poly(Acrylic Acid) Complexes. *Macromolecules* **2016**, *49*, 7563−7570.
(54) Reisch, A.; Roger, E.; Phoeung, T.; Antheaume, C.; Orthlieb, C.; Boulmedais, F.; Lavalle, P.; Schlenoff, J. B.; Frisch, B.; Schaaf, P. On the Benefits of Rubbing Salt in the Cut: Self-Healing of Saloplastic PAA/PAH Compact Polyelectrolyte Complexes. *Adv. Mater.* **2014**, *26*, 2547−2551.
(55) Zhao, M.; Xia, X.; Mao, J.; Wang, C.; Dawadi, M. B.; Modarelli, D. A.; Zacharia, N. S. Composition and Property Tunable Ternary Coacervate: Branched Polyethylenimine and a Binary Mixture of a Strong and Weak Polyelectrolyte. *Mol. Syst. Des. Eng.* **2019**, *4*, 110−121.
(56) Chollakup, R.; Smitthipong, W.; Eisenbach, C. D.; Tirrell, M. Phase Behavior and Coacervation of Aqueous Poly(Acrylic Acid)-Poly(Allylamine) Solutions. *Macromolecules* **2010**, *43*, 2518−2528.
(57) Fu, J.; Fares, H. M.; Schlenoff, J. B. Ion-Pairing Strength in Polyelectrolyte Complexes. *Macromolecules* **2017**, *50*, 1066−1074.
(58) Weidman, J. L.; Mulvenna, R. A.; Boudouris, B. W.; Phillip, W. A. Unusually Stable Hysteresis in the PH-Response of Poly(Acrylic Acid) Brushes Confined within Nanoporous Block Polymer Thin Films. *J. Am. Chem. Soc.* **2016**, *138*, 7030−7039.
(59) Petrov, A. I.; Antipov, A. A.; Sukhorukov, G. B. Base-Acid Equilibria in Polyelectrolyte Systems : From Weak Polyelectrolytes to Interpolyelectrolyte Complexes and Multilayered Polyelectrolyte Shells. *Macromolecules* **2003**, *36*, 10079−10086.
(60) Lappan, U.; Wiesner, B.; Scheler, U. Segmental Dynamics of Poly(Acrylic Acid) in Polyelectrolyte Complex Coacervates Studied

https://dx.doi.org/10.1021/acs.macromol.0c00999
Macromolecules 2020, 53, 7835−7844

by Spin-Label EPR Spectroscopy. *Macromolecules* **2016**, *49*, 8616−8621.
(61) Perry, S.; Li, Y.; Priftis, D.; Leon, L.; Tirrell, M. The Effect of Salt on the Complex Coacervation of Vinyl Polyelectrolytes. *Polymers* **2014**, *6*, 1756−1772.
(62) Huang, S.; Zhao, M.; Dawadi, M. B.; Cai, Y.; Lapitsky, Y.; Modarelli, D. A.; Zacharia, N. S. Effect of Small Molecules on the Phase Behavior and Coacervation of Aqueous Solutions of Poly-(Diallyldimethylammonium Chloride) and Poly(Sodium 4-Styrene Sulfonate). *J. Colloid Interface Sci.* **2018**, *518*, 216−224.
(63) Aberkane, L.; Jasniewski, J.; Gaiani, C.; Scher, J.; Sanchez, C. Thermodynamic Characterization of Acacia Gum-β-Lactoglobulin Complex Coacervation. *Langmuir* **2010**, *26*, 12523−12533.
(64) Zhao, M.; Zacharia, N. S. Sequestration of Methylene Blue into Polyelectrolyte Complex Coacervates. *Macromol. Rapid Commun.* **2016**, *37*, 1249−1255.
(65) Wang, S.; Chen, K.; Kayitmazer, A. B.; Li, L.; Guo, X. Tunable Adsorption of Bovine Serum Albumin by Annealed Cationic Spherical Polyelectrolyte Brushes. *Colloids Surf., B* **2013**, *107*, 251−256.
(66) Wang, Q.; Schlenoff, J. B. The Polyelectrolyte Complex/Coacervate Continuum. *Macromolecules* **2014**, *47*, 3108−3116.
(67) Zhang, Y.; Yildirim, E.; Antila, H. S.; Valenzuela, L. D.; Sammalkorpi, M.; Lutkenhaus, J. L. The Influence of Ionic Strength and Mixing Ratio on the Colloidal Stability of PDAC/PSS Polyelectrolyte Complexes. *Soft Matter* **2015**, *11*, 7392−7401.
(68) Priftis, D.; Farina, R.; Tirrell, M. Interfacial Energy of Polypeptide Complex Coacervates Measured via Capillary Adhesion. *Langmuir* **2012**, *28*, 8721−8729.
(69) Li, L.; Srivastava, S.; Andreev, M.; Marciel, A. B.; De Pablo, J. J.; Tirrell, M. V. Phase Behavior and Salt Partitioning in Polyelectrolyte Complex Coacervates. *Macromolecules* **2018**, *51*, 2988−2995.
(70) Zhang, P.; Shen, K.; Alsaifi, N. M.; Wang, Z.-G. Salt Partitioning in Complex Coacervation of Symmetric Polyelectrolytes. *Macromolecules* **2018**, *51*, 5586−5593.
(71) Lytle, T. K.; Sing, C. E. Tuning Chain Interaction Entropy in Complex Coacervation Using Polymer Stiffness, Architecture, and Salt Valency. *Mol. Syst. Des. Eng.* **2018**, *3*, 183−196.
(72) Mu, M.; Rieser, T.; Lunkwitz, K.; Meier-haack, J. Polyelectrolyte Complex Layers: A Promising Concept for Anti- Fouling Coatings Verified by in-Situ ATR-FTIR Spectroscopy. *Macromol. Rapid Commun.* **1999**, *20*, 607−611.
(73) Cranford, S. W.; Ortiz, C.; Buehler, M. J. Mechanomutable Properties of a PAA / PAH Polyelectrolyte Complex: Rate Dependence and Ionization Effects on Tunable Adhesion Strength. *Soft Matter* **2010**, *6*, 4175−4188.
(74) Rathee, V. S.; Zervoudakis, A. J.; Sidky, H.; Sikora, B. J.; Whitmer, J. K. Weak Polyelectrolyte Complexation Driven by Associative Charging. *J. Chem. Phys.* **2018**, *148*, 114901.
(75) Rathee, V. S.; Sidky, H.; Sikora, B. J.; Whitmer, J. K. Role of Associative Charging in the Entropy-Energy Balance of Polyelectrolyte Complexes. *J. Am. Chem. Soc.* **2018**, *140*, 15319−15328.
(76) Flory, P. J.; Osterheld, J. E. Intrinsic Viscosities of Polyelectrolytes. Poly-(Acrylic Acid). *J. Phys. Chem.* **1954**, *58*, 653−661.
(77) Buscall, R.; Corner, T. The Phase Separation Behaviour of Aqueous Solutions of Polyacrylic Acid and Its Partial Sodium Salts in the Presence of Sodium Chloride. *Eur. Polym. J.* **1982**, *18*, 967−974.
(78) Prabhu, V. M.; Muthukumar, M.; Wignall, G. D.; Melnichenko, Y. B. Polyelectrolyte Chain Dimensions and Concentration Fluctuations near Phase Boundaries. *J. Chem. Phys.* **2003**, *119*, 4085−4098.
(79) Thakur, A.; Wanchoo, R. K.; Singh, P. Structural Parameters and Swelling Behavior of PH Sensitive Poly(Acrylamide-Co-Acrylic Acid) Hydrogels. *Chem. Biochem. Eng. Q.* **2011**, *25*, 181−194.
(80) Eustace, D. J.; Siano, D. B.; Drake, E. N. Polymer Compatibility and Interpolymer Association in the Poly(Acrylic Acid)−Polyacrylamide−Water Ternary System. *J. Appl. Polym. Sci.* **1988**, *35*, 707−716.
(81) Borue, V. Y.; Erukhimovich, I. Y. A Statistical Theory of Weakly Charged Polyelectrolytes: Fluctuations, Equation of State and Microphase Separation. *Macromolecules* **1988**, *21*, 3240−3249.
(82) Ou, Z.; Muthukumar, M. Entropy and Enthalpy of Polyelectrolyte Complexation: Langevin Dynamics Simulations. *J. Chem. Phys.* **2006**, *124*, 154902.
(83) Ting, J. M.; Wu, H.; Herzog-Arbeitman, A.; Srivastava, S.; Tirrell, M. V. Synthesis and Assembly of Designer Styrenic Diblock Polyelectrolytes. *ACS Macro Lett.* **2018**, *7*, 726−733.
(84) Hunt, J. N.; Feldman, K. E.; Lynd, N. A.; Deek, J.; Campos, L. M.; Spruell, J. M.; Hernandez, B. M.; Kramer, E. J.; Hawker, C. J. Tunable, High Modulus Hydrogels Driven by Ionic Coacervation. *Adv. Mater.* **2011**, *23*, 2327−2331.
(85) Srivastava, S.; Levi, A. E.; Goldfeld, D. J.; Tirrell, M. V. Structure, Morphology, and Rheology of Polyelectrolyte Complex Hydrogels Formed by Self-Assembly of Oppositely Charged Triblock Polyelectrolytes. *Macromolecules* **2020**, *53*, 5763−5774.

https://dx.doi.org/10.1021/acs.macromol.0c00999
Macromolecules 2020, 53, 7835−7844